RAPID COMMUNICATIONS

PHYSICAL REVIEW B VOLUME 42, NUMBER 5 15 AUGUST 1990-I

Resonant-Raman-scattering studies of disorder in solution-cast polydiacetylene films

L. X. Zheng, R. E. Benner, and Z. V. Vardeny
Department of Physics, Department of Electrical Engineering, and University of Utah Laser Institute, University of Utah, Salt Lake City, Utah 84112

G. L. Baker
Communications Research, Incorporated, 331 Newman Springs Road, P. O. Box 7040, Red Bank, New Jersey 07701-7040
(Received 24 May 1990)

The disorder in polydiacetylene films cast from solution is studied by Raman scattering under preresonance and resonance conditions in both Stokes and anti-Stokes configurations. The disorder-induced inhomogeneities in the exciton energy levels and the strongly coupled vibrations cause strong dispersion of the C=C and C≡C stretching frequencies with the laser excitation photon energy, surprisingly similar to that of *trans*-polyacetylene. We show, however, that the complete inhomogeneously broadened phonon distribution is revealed when the excitation is not in resonance. In addition to the excitation resonance, resonances associated with the Stokes and anti-Stokes emission beams strongly affect the measured Raman profiles.

Resonant Raman scattering (RRS) is an efficient method for studying disorder in conducting polymers since the inhomogeneously broadened distribution of phonon frequencies caused by the disorder is selectively probed by changing the excitation laser photon energy $\hbar\omega_L$.[1-9] The resonant enhancement causes the frequencies of the most strongly coupled Raman-active phonons to shift with ω_L; this phenomenon is known as phonon dispersion. The RRS dispersion in polyacetylene [$(CH)_x$] has been the focus of experimental and theoretical studies for the last decade[1-3,5-9] because of the relative simplicity of the polymer backbone structure, the measured large phonon dispersion, and the convenient laser excitation range (in the visible and near uv spectrum). Two competing models, an heuristic distribution of chain lengths[6] and the amplitude modes model,[5,8] can explain well the RRS dispersive spectra in various isomers and doped forms of $(CH)_x$. Recently, a successful attempt was made[10] to unify these two theories into a single model. It is now generally believed that the electron interactions and consequently the energy gap in $(CH)_x$ are dominated by the electron-phonon (e-p) coupling and that the disorder in the films causes an inhomogeneous distribution of the e-p coupling through a distribution of conjugation lengths.[10] Polydiacetylene (PDA), on the other hand, is believed to be dominated by stronger electron-electron (e-e) interactions. A comparison between the RRS dispersion in PDA and that of $(CH)_x$ may reveal new information on the relative importance of these interactions. Also PDA exhibits exceptional electronic and optical properties which include high nonlinear optical constants[11] and strong exciton-phonon coupling;[12,13] both properties stem from the strong one-dimensional (1D) anisotropy of this material. Moreover, optical-quality PDA thin films[14] can be easily prepared by the technique of spin casting from solution, and is also the first conjugated polymer to form a real all-optical device.[15]

In this paper we present RRS studies of the disorder in PDA [poly(4-butoxycarbonyl-methylurethane) (4-BCMU)] films. We show that under resonant conditions, the Stokes (S) as well as the anti-Stokes (AS) Raman frequencies of the C=C and C≡C stretching vibrations exhibit strong dispersion with ω_L surprisingly similar to that in *trans*-$(CH)_x$. We also show that the complete disorder-induced phonon distribution is directly revealed when ω_L is not in resonance. By measuring the S- to AS-intensity ratio as a function of ω_L, we demonstrate the importance of the resonance enhancement with the scattered (outgoing) beam; this effect has not been taken into account in any of the existing theories concerning RRS dispersion in conducting polymers.

Large-area PDA 4-BCMU films of thicknesses between 1000 and 8000 Å were prepared by spin casting from solution onto sapphire substrates.[14] Some of the films were further annealed at temperatures near the 4-BCMU disordering temperature (~115 °C) to vary their inhomogeneity and disorder. Raman-scattering data were recorded in a transmission-scattering geometry using various excitation lasers including He-Ne, Ar^+, Ar^+-pumped dye [in the Rhodamine-6G and DCM, or 4-(dicyanomethylene)-2-(methyl-6-(*p*-dimethyl)-amino-styryl)-4*H*-pyran, dye spectral ranges], frequency-doubled neodymium-doped yttirum aluminum garnet (Nd:YAG) and Ar^+-pumped Ti: sapphire lasers. Irradiance levels at the PDA samples were kept below 10^4 W/cm^2 to suppress light-induced defects in the films. Scattered radiation was collected at $f/1.2$ using an achromatic lens combination and was focused onto the entrance slit of a triple spectrograph equipped with 300-, 600-, or 1200-groove/mm ruled gratings. We have used optical multichannel detection with a cooled CCD (Thomson-CSF) having an array of 384×576 picture elements (pixels), each with dimensions of 23×23 μm^2; this corresponds to about 1 cm^{-1} resolution/pixel using the 1200-groove/mm grating in the red visible range. Depending upon ω_L, spectra were recorded with exposure times ranging from 10 to 200 sec for ω_L in resonance and 10–30 min when ω_L was not in resonance. For the 4-BCMU films resonance conditions

were achieved for $1.9 \leq \omega_L \leq 2.4$ eV; this is in the absorption *tail* of the PDA films, in contrast to $(CH)_x$ where resonant conditions are usually observed when ω_L is *above* the film absorption maximum.[1-3]

The complete RRS spectrum of the PDA films contains about eight resonantly enhanced phonon lines. We found, however, that strong dispersion only occurs in the C=C ($\omega_3 \simeq 1500$ cm^{-1}) and C≡C ($\omega_4 \simeq 2100$ cm^{-1}) stretching vibrations. Typical RRS spectra of the C=C stretching vibration (ω_3) for various excitations ω_L in Stokes and anti-Stokes configurations are shown in Fig. 1. From $\alpha(\omega)$ given in Fig. 2(c), resonance scattering occurs for $\omega_L \geq 1.9$ eV. Under these conditions strong dispersion in ω_3 in both S and AS configurations is observed when ω_L increases. We note, however, that for each ω_L, $\omega_3(S) \neq \omega_3(AS)$ and the S and AS spectra exhibit different line-shape characteristics. For $\omega_L = 1.88$ eV, the excitation beam is in preresonance [Fig. 2(c)] and Fig. 1 shows that a very broad S Raman line (width of about 60 cm^{-1}) is obtained; this line essentially contains all ω_3 Raman frequencies which are excited at ω_L in resonance and, thus, it reveals the complete inhomogeneously broadened phonon distribution in the sample. It is quite remarkable that a *single* experiment, Raman scattering in preresonance condition, can quite accurately reveal the inhomogeneity in PDA samples. We have checked the feasibility of this method for various samples of PDA prepared or annealed under different conditions. In all cases the preresonant spectrum was quite sufficient to detect the different degree of disorder.

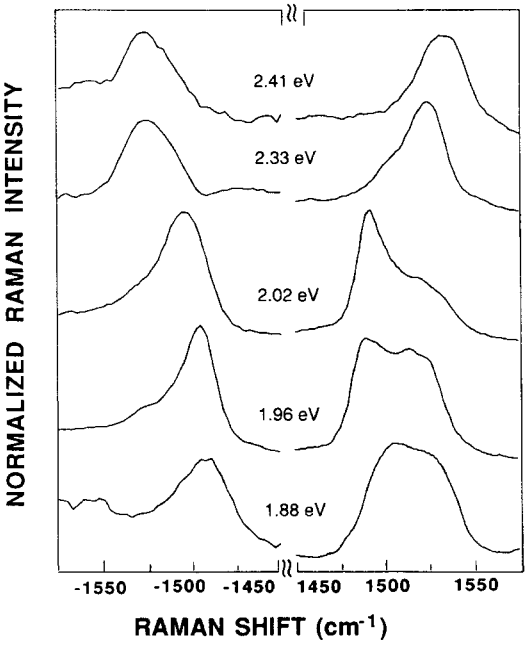

FIG. 1. Resonant-Raman-scattering spectra from the C=C stretching vibrations in polydiacetylene 4-BCMU films, in the Stokes ($+\omega$) and anti-Stokes ($-\omega$) configurations, for various excitation photon energies. The Stokes 1.88-eV spectrum is not excited in resonance and thus the whole distribution of the C=C stretching vibrations is observed.

The frequency dispersion with ω_L is summarized in Fig. 2 for the (a) C=C and (b) C≡C stretching vibrations for both S and AS configurations. We attribute this dispersion to a resonance Raman process in which different portions of the inhomogeneously broadened phonon distribution are selectively enhanced by resonances at ω_L, or at either the S ($\omega_L - \omega_R$) or the AS ($\omega_L + \omega_R$) emission (outgoing) beams. The S data in preresonance ($\omega_L < 1.9$ eV) reveal the entire inhomogeneous distribution (Fig. 1) and, therefore, ω_3 peaks in the middle of the frequency dispersion in Fig. 2(a) ($\bar{\omega}_3 \simeq 1512$ cm^{-1}). As ω_L increases, ω_3(S) shows evidence of selective resonant enhancement. We note that this occurs in PDA for ω_L at or below the pronounced exciton band in $\alpha(\omega)$ [ω_x in Fig. 2(c)] and, therefore, the disorder in the electronic bands in PDA is probably associated with the distribution in the 1D exciton levels, not with E_g as is the case in $(CH)_x$. For $\omega_L > 2.5$ eV the excitation laser is beyond resonance, but the frequency-shifted S emissions ($\omega_L - \omega_3$) are near resonance. Consequently, ω_3(S) decreases and moves towards the center of the phonon distribution [Fig. 2(a)]. We also note from Fig. 2(a) that $\bar{\omega}_3$ at the center of the phonon distribution is selectively enhanced at $\omega_L = 2.25$

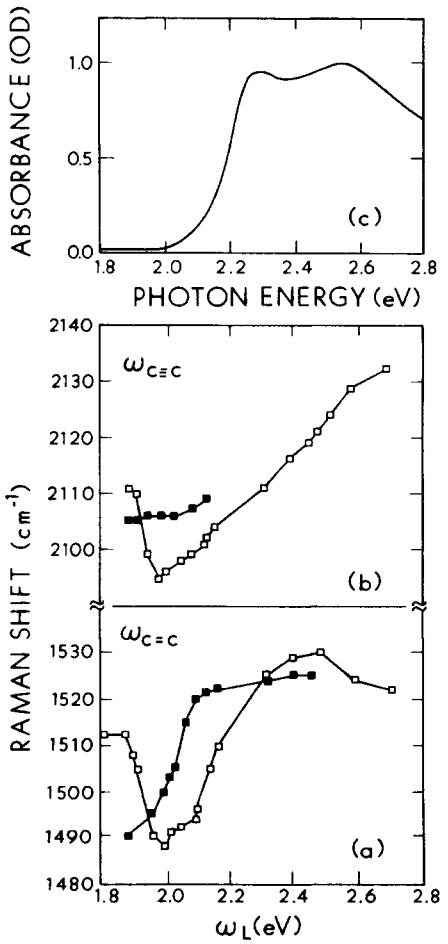

FIG. 2. Stokes (□) and anti-Stokes (■) RRS dispersion with ω_L for the (a) C=C and (b) C≡C stretching vibrations of PDA. (c) The PDA film's optical density (OD) spectrum $\alpha(\omega)d$, showing the dominant exciton band at $\omega_x \simeq 2.25$ eV.

eV, which is the exciton absorption band maximum ω_x [Fig. 2(c)]. This further confirms that the disorder in the exciton levels is the underlying mechanism for the RRS dispersion in PDA.

The AS C=C data [Fig. 2(a)] are consistent with the S data interpretation, but the dominant resonance is associated with the AS emission at $\omega_L+\omega_3$, rather than with ω_L. As ω_L increases, portions of the inhomogeneously broadened phonon distribution are again resonantly enhanced, but ω_3(AS) is greater than ω_3(S) (Fig. 1) corresponding to resonance at $\omega_L+\omega_3$, not at ω_L. Indeed, as evident in Fig. 2(a) the dispersion in ω_3(AS) is shifted to lower ω_L with respect to the dispersion in ω_3(S) by about 0.19 eV ($\simeq\bar{\omega}_3$), but deviations caused by variations in the relative contributions of ω_L and $\omega_L+\omega_3$ resonances are also evident.

Figure 2(b) shows the measured dispersion in the C≡C stretching frequency ω_4 in S and AS configurations. Because of the larger value of ω_4, it was more difficult to obtain data for AS and, therefore, only data at full resonance, where $\omega_L+\omega_4\simeq 2.3$ eV, are shown. Again, we see preresonance for $\omega_L \leq 1.9$ eV and a monotonic increase in ω_4 for $\omega_L > 2$ eV. We note, however, that the dispersion in ω_4 does not saturate as for ω_3(S) [Fig. 2(a)] because the S emission at $\omega_L-\omega_4$ is not in full resonance even at the highest ω_L attained.

The dependence of the measured AS- to S-Raman-intensity ratio on ω_L is shown in Fig. 3 for the C=C vibration. The measured ratios, corrected for the spectrometer response, vary over more than 3 orders of magnitude with ω_L. Since the Raman data in Fig. 1 are normalized to be of equal intensity, the S and AS intensity differences are not plotted. Nevertheless, the nearly equal signal-to-noise ratios observed for S and AS peaks at some excitation energies is surprising since the room-temperature Boltzmann factor for $\omega_3=1500\ \mathrm{cm}^{-1}$ is $\sim 8\times 10^{-4}$. This value for the AS- to S-intensity ratio is expected when both the AS and S peaks are not in resonance. At $\omega_L=1.9$ eV in Fig. 3, the S and AS peaks are in preresonance and a value for the AS- to S-intensity near the Boltzmann factor is observed. As ω_L increases, the AS intensity initially increases because of the AS emission resonance at $\omega_L+\omega_3$. The intensity ratio increases to a maximum value of ~ 0.4 near 2.0 eV, when $\omega_L+\omega_3$ are close to ω_x. For $\omega_L > 2.0$ eV, the excitation energy is coming into resonance resulting in an increasing S intensity and the AS emission resonance is decreasing resulting in a lower AS- to S-intensity ratio. For $\omega_L\simeq 2.5$ eV, the S emission is near resonance at $\omega_L-\omega_3\simeq\omega_x$ which causes the S intensity to be optimally enhanced and consequently the AS- to S-intensity ratio becomes lower than the Boltzmann value. These results show the importance of the resonances associated with the outgoing Raman-scattering beams at $\omega_L\pm\omega_3$. From Fig. 3 we estimate the resonant enhancement to be about 10^3. This resonance process has not yet been taken into account in any theory of RRS in conducting polymers[6-9] and our results prove that it cannot be neglected.

A crucial test to identify the type of disorder underlying the RRS dispersion in conducting polymers is provided by the disorder amplitude-mode (AM) model.[8] A powerful relation is the multiplication rule $\prod_i(\omega_R^i)^2\sim 2\tilde{\lambda}$, where ω_R^i are the Raman frequencies of all A_g lines which are resonantly enhanced at ω_L and $\tilde{\lambda}(\omega_L)$ is the renormalization parameter for the AM frequencies at ω_L. Using this relation, we plot in Fig. 4 $\prod_i(\omega_p^i/\omega_s^i)^2$ vs $\ln(\hbar\omega_L)$, where ω_p^i and ω_s^i are all eight RRS frequencies at $\omega_L=\omega_x=2.25$ eV (P) and at ω_L (S), respectively. The above RRS frequencies ratio is proportional[8] to $[\tilde{\lambda}(\omega_L)]^{-1}$ and, thus, Fig. 4 shows that $(\tilde{\lambda})^{-1}$ is proportional to $-\ln(\hbar\omega_L)$, surprisingly similar to the case of *trans*-$(CH)_x$.[5,8] The deviation from the straight line seen in Fig. 4 at high ω_L is caused by $\omega_L-\omega_R$ resonances, as explained before for Fig. 2(a). Moreover, from a complete fit to the RRS data using the AM model to find $\tilde{\lambda}$ and ω_0^i (bare frequencies) in a similar way as for *trans*-$(CH)_x$,[8] we obtained[16] the relation

$$\tilde{\lambda}_p/\tilde{\lambda}(\omega_L)=1-0.51\ln(\omega_L/\omega_x),$$

where $\tilde{\lambda}_p$ is $\tilde{\lambda}$ at ω_x. The AM analysis shows a Peierls-

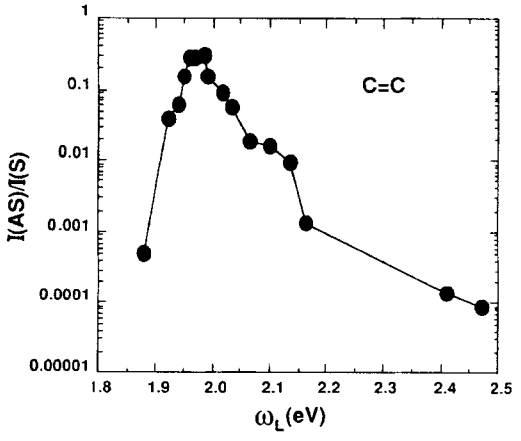

FIG. 3. AS- to S-Raman intensities ratio of the C=C stretching vibrations vs the excitation photon energy ω_L. The nonresonant (Boltzmann) intensities ratio is 8×10^{-4}.

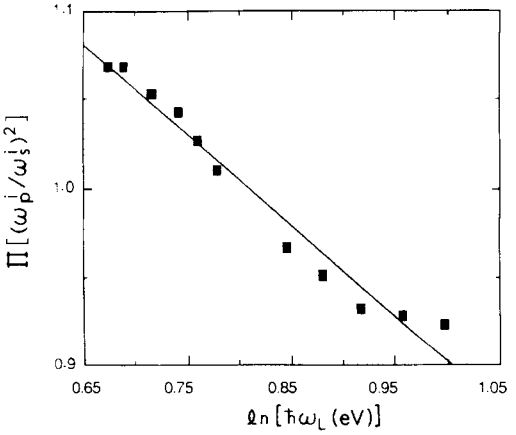

FIG. 4. The multiplication ratio $\prod_i(\omega_p^i)^2/\prod_i(\omega_s^i)^2$ for all 8 RRS vibrations in PDA films, where p denotes excitation at $\omega_L=\omega_x$ (the exciton band) and s stands for any ω_L, vs $\ln(\hbar\omega_L)$. The straight line is a theoretical fit to the data using a Peierls-type relation.

type relation for E_g with $E_g \sim \exp(-1/2\lambda)$ and $\tilde{\lambda} = \lambda$, the e-p coupling. According to this model,[8] the ordered $2\lambda_p = 2\lambda_p = 0.51$ and the inhomogeneity occurs in λ, which in turn broadens the distribution in the electronic energies (and E_x) and in the Raman-active phonon frequencies ω_R. Since PDA is believed to exhibit stronger e-e interactions than $(CH)_x$, it is surprising to see such a good fit with the Peierls relation, which is based only on e-p interaction. On the other hand, the similarity with *trans*-$(CH)_x$ may indicate that the same type of disorder exists in both materials. Since the interaction parameters ultimately depend on the conjugation length N,[10] we believe that a distribution of conjugation lengths is the underlying mechanism for the RRS dispersion in both PDA and $(CH)_x$. In PDA it causes inhomogeneity in the exciton energies E_x, in $(CH)_x$ it is E_g which varies with N. However, ω (N) in both materials is similar. More theoretical work is needed to elucidate these points.

In summary, we have investigated RRS in PDA 4-BCMU films cast from solution. The disorder-induced distributions in the exciton levels and the C=C and C≡C stretching vibrations cause strong dispersion of these phonon frequencies with ω_L in both S and AS configurations. We showed, however, that a single experiment, when ω_L is not in resonance, reveals the complete inhomogeneous broadened phonon distribution and can serve as a standard method to probe the amount of disorder in PDA films. We have also demonstrated the importance of resonances with the outgoing (scattered) beams for both S $(\omega_L - \omega_R)$ and AS $(\omega_L + \omega_R)$ configurations. Finally, we have pointed out the similarity in the types of disorder in PDA and *trans*-$(CH)_x$, as revealed by the AM analysis of the RRS dispersion.

This work was partially supported by U.S. Department of Energy Grant No. DE-FG02-89ER45409, and by the Free Electron Laser program at the University of Utah.

[1]I. Harada, Y. Furukawa, M. Tasumi, H. Shirakawa, and S. Ikeda, J. Chem. Phys. **73**, 4746 (1980).

[2]L. S. Lichtman, A. Sarhangi, and D. B. Fitchen, Solid State Commun. **36**, 869 (1980).

[3]H. Kuzmany, Phys. Status Solidi B **97**, 521 (1980).

[4]M. L. Shand, R. R. Chance, M. LePostollec, and M. Schott, Phys. Rev. B **25**, 4431 (1982).

[5]Z. Vardeny, E. Ehrenfreund, O. Brafman, and B. Horovitz, Phys. Rev. Lett. **51**, 2326 (1983); **54**, 75 (1985).

[6]G.P. Brivio and E. Mulazzi, Phys. Rev. B **30**, 876 (1984).

[7]E. Faulques, E. Rzepka, S. Lefrant, E. Mulazzi, G. P. Brivio, and G. Leising, Phys. Rev. B **33**, 8622 (1986).

[8]E. Ehrenfreund, Z. Vardeny, O. Brafman, and B. Horovitz, Phys. Rev. B **36**, 1535 (1987).

[9]C. Castiglioni, J. T. Lopez Navarrete, G. Zerbi, and M. Gussoni, Solid State Commun. **65**, 625 (1988).

[10]M. Gussoni, C. Castiglioni, and G. Zerbi, Synth. Met. **28**, D375 (1989).

[11]G. Carter, J. Hryniewicz, M. Thakur, Y. Chen, and S. Meyler, Appl. Phys. Lett. **49**, 998 (1986).

[12]B. I. Greene, J. F. Mueller, J. Orenstein, D. H. Rapkine, S. Schmitt-Rink, and M. Thakur, Phys. Rev. Lett. **61**, 325 (1988).

[13]G. L. Blanchard, J. P. Heritage, A. C. vonLehmen, M. K. Kellog, G. L. Baker, and S. Etemad, Phys. Rev. Lett. **63**, 887 (1989).

[14]P. D. Townsend, G. L. Baker, N. E. Schlotter, C. F. Klausner, and S. Etemad, Appl. Phys. Lett. **53**, 1782 (1988).

[15]P. D. Townsend, G. L. Baker, N. E. Schlotter, and S. Etemad, Synth. Met. **28**, 633 (1989); **28**, 639 (1989).

[16]L. X. Zheng, R. E. Benner, Z. V. Vardeny, and G.L. Baker (unpublished).